Suspended microchannel resonators for biomolecular detection

T. P. Burg[a] and S. R. Manalis[b]
Massachusetts Institute of Technology, Media Laboratory, 20 Ames Street, Cambridge, Massachusetts 02139

(Received 27 June 2003; accepted 31 July 2003)

We present a resonant mass sensor for specific biomolecular detection in a subnanoliter fluid volume. The sensing principle is based on measuring shifts in resonance frequency of a suspended microfluidic channel upon accumulation of molecules on the inside walls of the device. Confining the fluid to the inside of a hollow cantilever enables direct integration with conventional microfluidic systems, significantly increases sensitivity by eliminating high damping and viscous drag, and allows the resonator to be actuated by electrostatic forces. Fluid density measurements reveal a mass resolution of 10^{-17} g/μm^2 in a 4 mHz–4 Hz bandwidth. To demonstrate biomolecular detection, we present real-time measurements of the specific binding between avidin and biotinylated bovine serum albumin. Based on these measurements, we expect that changes in surface mass loading on the order of 10^{-19} g/μm^2 can be detected in an optimized system. [DOI: 10.1063/1.1611625]

Label-free detectors for biomolecules in solution have great potential for improving the throughput and utility of assays for pharmaceutical and biological research as well as for medical diagnostics and environmental monitoring. While fluorescent and radioactive labeling methods provide high sensitivity, the necessary sample preparation and the modification of the molecules of interest are often undesirable. Label-free alternatives such as surface plasmon resonance (SPR) sensors and quartz crystal microbalances (QCM) eliminate the need for chemical modification by providing a direct measure of surface binding based on the intrinsic properties of the molecules. However, the QCM and SPR sensors are significantly less sensitive than fluorescence, they require large sample volumes (typically in the 10–1000 μL range) and are generally difficult to scale (both down in size and up in number) without degrading sensitivity. As a result, their utility for biological applications is often limited.

There are several emerging approaches based on microfabrication that are aimed at addressing these limitations. Recent examples include field-effect sensors,[1–3] integrated optics[4,5] and surface stress sensors.[6–8] Resonant beam mass sensors, while successful for chemical sensing in gaseous environments,[9–11] have received less attention for biomolecular detection in solution. This is primarily because the mass sensitivity and frequency resolution are significantly degraded by the low quality factor and large effective mass that is induced by viscous drag. While the quality factor can be enhanced by using electronic feedback known as Q control,[12,13] the mass sensitivity, in terms of frequency shift per mass loading, is not improved.

In this letter, we show that the problems of damping and viscous drag associated with a resonant beam mass sensor in fluid can be circumvented by confining the fluid to the inside of the resonant beam while leaving the channel exterior in a gaseous environment, or vacuum [Fig. 1(a)]. Since the mass density of biological molecules is greater than the mass density of the fluid (e.g., proteins typically range from 1.3 to 1.4 g/cm^3),[14] the resonance frequency of the suspended microchannel is decreased by the adsorption of molecules to the channel walls. This is illustrated schematically in Fig. 1(b). To detect specific biomolecules, the channel walls are first functionalized with a layer of capture molecules. Subsequent accumulation of target molecules on the functionalized walls decreases the resonance frequency.

The device with internal surface area A can be modeled as a harmonic oscillator with an effective mass m and resonance frequency f. The relative frequency shift $\Delta f/f$ resulting from a small surface mass loading $\Delta\sigma=\Delta m/A$ is given to first order by

$$\frac{\Delta f}{f}=-\frac{1}{2}\left(\frac{A}{m}\right)\cdot\Delta\sigma. \tag{1}$$

Equation (1) shows that for a given detectable frequency shift Δf and a resonance frequency f, the smallest detectable surface mass loading is fully determined by the ratio of surface area to total mass. This ratio can be improved by reducing the thickness of the fluid layer as well as that of the channel walls.

Various processes for fabricating suspended microchannels designed for measuring volumetric mass density have been reported earlier.[15,16] As described earlier, suspended microchannels for biomolecular detection must be sufficiently thin, and additionally they must be configured for continuous fluidic delivery for real-time measurements. To address both of these requirements, we combined a polysilicon Damascene process, sacrificial layer etching in hot potassium hydroxide,[17] and bulk micromachining to fabricate suspended microchannels with a wall thickness of 800 nm and a fluid layer thickness of 1.2 μm. The fabrication starts by etching the microfluidic channels in a standard ⟨100⟩ silicon wafer using photolithography and reactive ion etching (RIE). The wafer is subsequently coated with 800 nm low-stress low-pressure chemical vapor deposited silicon nitride and 1.5 μm polysilicon, followed by planarization with chemical mechanical polishing (CMP). The CMP process is timed to

[a]Also at: Department of Electrical Engineering and Computer Science, Massachusetts Institute of Technology.
[b]Also at: Division of Biological Engineering, Massachusetts Institute of Technology; electronic mail: scottm@media.mit.edu

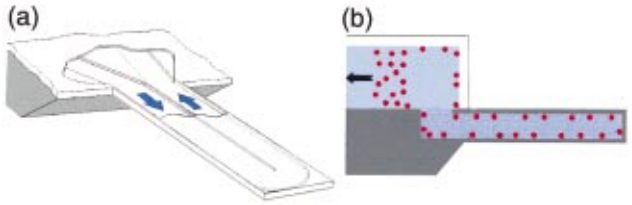

FIG. 1. (Color) (a) High damping and the large effective mass in liquid phase resonant mass sensors are avoided by using suspended microfluidic channels as resonators. (b) Analytes are detected based on their mass density difference relative to the surrounding solution.

stop as soon as it reaches the silicon nitride layer so that the channels remain filled with polysilicon. After the CMP, a second layer of low-stress silicon nitride with the same thickness as the first layer is deposited. This layer closes the microfluidic channels, which are now filled with polysilicon. Again, standard photolithography and RIE are used to pattern the two silicon nitride layers in order to define the outline of the resonators as well as access ports to the insides of the channels. The wafer backside is also patterned in the same step to define the locations of through-holes under the suspended sections of the channel. Finally, the sacrificial polysilicon and the wafer through-holes are etched in a 6 M aqueous potassium hydroxide solution at 80 °C. We found that at this temperature, diffusion does not severely limit the etch rate for the sacrificial layer. We were able to completely release channels up to 1 mm in less than 20 h with a yield of 80%.

An electron micrograph of three suspended microchannels is shown in Fig. 2(a), and a phase contrast optical image is shown in Fig. 2(b). To obtain continuous fluidic delivery to the suspended channels, a microfluidic network made of

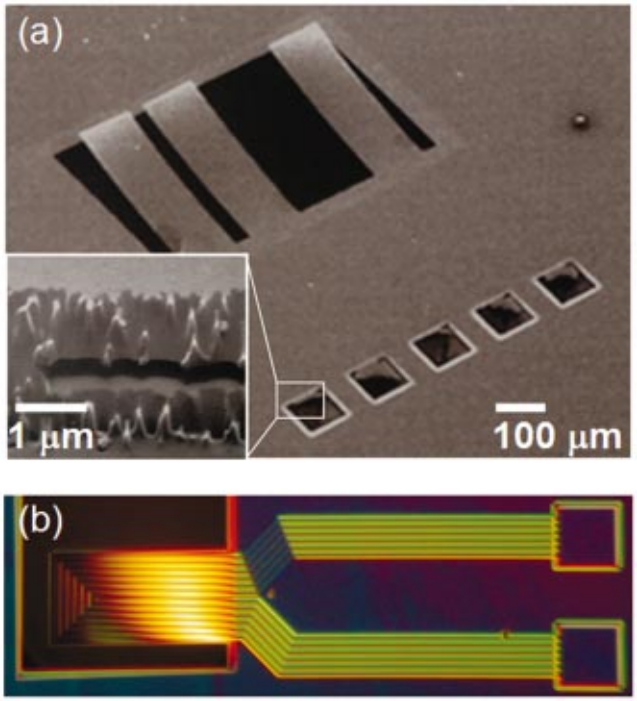

FIG. 2. (a) (Color) Suspended microfluidic channels up to 500 μm in length were fabricated using a polysilicon sacrificial layer process. The inset shows a channel with a height of 500 nm. (b) The optical micrograph shows a single 300 μm long cantilever holding six parallel fluid channels.

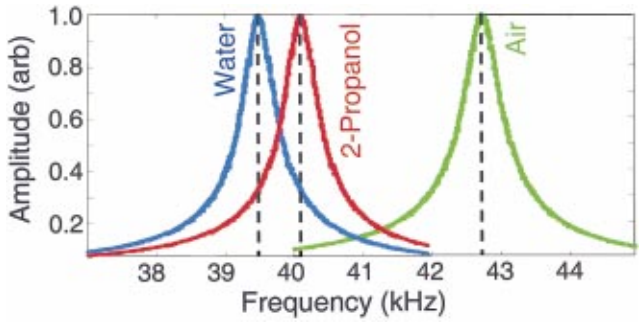

FIG. 3. (Color) The normalized frequency response curves of a 300 μm long cantilever filled with air, 2-propanol and water are shown. The three center frequencies are 42.7, 40.1, and 39.6 kHz, respectively The mechanical quality factor in air is ~90 and does not depend on the filling medium.

poly(dimethylsiloxane) (PDMS) was bonded to the chip surface. The inlets to the nitride channels were located within U-shaped channels in the PDMS so that solutions could be transported with low flow resistance to the low-volume microchannels. The device was actuated electrostatically, and the deflection was measured with the optical lever method. Good electrical conductivity and high optical reflectivity were achieved by coating the suspended channels with a 100 nm aluminum thin film. The aluminum was connected to ground, and a drive electrode was brought to within 50 μm of the device by means of a micrometer stage.

Frequency responses were recorded using a function generator in frequency sweep mode and a lock-in amplifier. To obtain time plots of the resonance frequency, the device was placed in a feedback loop, with the output of the deflection sensor connected directly to the drive electrode via a saturating voltage amplifier with ± 5 V output swing. The drive signal was offset by $+60$ V with respect to ground, and the oscillation frequency was measured by means of an HP53131A frequency counter. In this configuration we observed a frequency noise level of 80 mHz rms in a 4 mHz–4 Hz measurement bandwidth.

In order to evaluate the mass resolution, we measured the frequency response for a 300 μm cantilever in the unfilled state, as well as filled with isopropyl alcohol, and filled with water. The resulting spectra are shown in Fig. 3. Taking into account the known mass densities of the different media and the design volume of 27 pL, we find a mass sensitivity of 107 mHz/pg for small loadings of a water filled microchannel. Given this sensitivity together with the 80 mHz noise

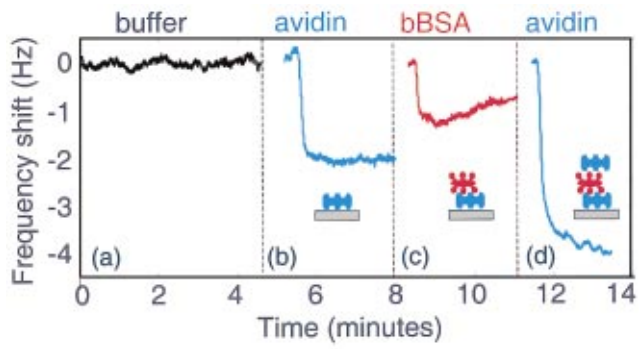

FIG. 4. (Color) The relative frequency shift for a 40 kHz resonant microchannel after injection of different solutions is shown for (a) buffer, (b) avidin, (c) bBSA, and (d) avidin.

level and a surface area of 53 000 μm^2, our current detection limit is approximately 1.4×10^{-17} g/μm^2 over a 4 mHz–4 Hz bandwidth.

We demonstrated biomolecular detection by functionalizing the interior channel walls with biotinylated bovine serum albumin (bBSA) and performing several experiments to detect the subsequent binding of avidin and bBSA. Constant fluid pressure was maintained at all times, except during the switching between reagents. Avidin and bBSA were dissolved in phosphate buffered saline at 500 μg/mL and 1 mg/mL, respectively. The results of these experiments are summarized in Fig. 4. Each section represents the relative frequency shift over time, zeroed at the point at which fluids were switched. Figure 4(a) shows the base line signal after disconnecting and reconnecting buffer. Figure 4(b) is the result of switching from buffer to avidin solution. The resonance frequency dropped sharply by more than 2 Hz a few seconds after changing fluids. This delay was expected due to the time required for the liquid to flow from the point of switching to the beginning of the suspended channel. When we switched back to buffer, the resonance frequency remained unchanged, indicating that fluid density difference did not cause the signal. Next, we verified that the frequency also remained unchanged when we reinjected avidin into the buffer filled microchannel. This suggests that all available binding sites for avidin had already been occupied. Next, we switched to bBSA solution, followed again by avidin. In both cases, a rapid drop in resonance frequency could be observed [Figs. 4(c) and 4(d)]. The fact that the injection of bBSA restored the ability to detect avidin in the resonating microchannel can be explained by bBSA-avidin multilayer formation, as illustrated schematically in Fig. 4. Since there are several biotins attached to each BSA molecule, a new bBSA layer (red symbols) can provide many binding sites for the subsequent adsorption of avidin (blue symbols).

None of the binding and control experiments described previously revealed frequency shifts from changes in volumetric density between buffer and bBSA or avidin. Although we estimate that these solutions should shift the frequency by a few hundred millihertz, we found that the complete exchange of fluid within the suspended microchannel often required several minutes. Over this time scale, frequency shifts below ~1 Hz would have been obscured by drift, which was often present. In contrast, the high binding affinity of biotin-avidin results in rapid saturation of the surface concentration even at a fraction of the volume concentration that we injected.

Our results demonstrate that the relatively large surface area to volume ratio of the microchannel is advantageous for mass detection. Once a dilute sample enters the microchannel, the molecules are quickly depleted as they bind to the immobilized capture molecules. As additional molecules enter, the surface soon collects many more molecules than are present in the surrounding solution. As a result, the enhanced channel concentration produces a measurable change in resonance frequency. This suggests that the binding signal could be significantly amplified through the use of three-dimensional surface coatings that improve the capture efficiency.

In conclusion, we have addressed the scaling and integration limitations of conventional label-free methods with a detection principle based on mechanically resonant microfluidic channels whereby the channels themselves are the detectors. We have demonstrated that a resonant channel of 27 pL volume can be integrated with conventional PDMS microfluidics, and in an unoptimized system, we have achieved a surface mass resolution of 10^{-17} g/μm^2, which is comparable to most commercial QCMs. We estimate that reducing the microchannel thickness and increasing resonance frequency by a factor of 3 will improve the sensitivity by tenfold, and based on previous frequency measurements of microcantilevers, we anticipate that improved environmental control will enhance frequency resolution by tenfold.[18] The combined improvements would result in a surface mass resolution of 10^{-19} g/μm^2, which is approximately equivalent to one protein per square micron. We envision that an array of suspended microchannel detectors with this resolution may provide an alternative to fluorescent-based detection for protein microarrays.

This work was supported by Defense Advanced Research Projects Agency (DARPA) Bio-Info-Micro Program, and Center for Bits and Atoms Contract No. CCR-0122419. The device was fabricated in MIT Microsystems Technology Laboratories. The authors thank R. Chakrabarti and M. Shusteff for providing valuable input in preparing this manuscript.

[1] J. Fritz, E. B. Cooper, S. Gaudet, P. K. Sorger, and S. R. Manalis, PNAS **99**, 14142 (2002).
[2] Y. Cui, Q. Wei, H. Park, and C. M. Lieber, Science **293**, 1289 (2001).
[3] R. J. Chen, S. Bangsaruntip, K. A. Drouvalakis, N. W. S. Kam, M. Shim, Y. Li, W. Kim, P. J. Utz, and H. Dai, PNAS **100**, 4984 (2002).
[4] J. Vörös, J. J. Ramsden, G. Csúcs, I. Szendrö, S. M. De Paul, M. Textor, and N. D. Spencer, Biomaterials **23**, 3699 (2002).
[5] W. Lukosz, Sens. Actuators B **29**, 37 (1995).
[6] J. Fritz, M. K. Baller, H. P. Lang, H. Rothuizen, P. Vettiger, E. Meyer, H. J. Güntherodt, Ch. Gerber, and J. K. Gimzewski, Science **288**, 316 (2000).
[7] G. Wu, R. H. Datar, K. M. Hansen, T. Thundat, R. J. Cote, and A. Majumdar, Nat. Biotechnol. **19**, 856 (2001).
[8] C. A. Savran, A. W. Sparks, J. Sihler, J. Li, W. C. Wu, D. E. Berlin, T. P. Burg, J. Fritz, M. A. Schmidt, and S. R. Manalis, J. Microelectromech. Syst. **11**, 703 (2002).
[9] D. Lange, C. Hagleitner, O. Brand, and H. Baltes, 14th Intl. Conf. Microelectromech. S., Interlaken, Switzerland, 2001.
[10] T. Thundat, E. A. Wachter, S. L. Sharp, and R. J. Warmack, Appl. Phys. Lett. **66**, 1695 (1995).
[11] M. Maute, S. Raible, F. E. Prins, D. P. Kern, H. Ulmer, U. Weimar, and W. Göpel, Sens. Actuators B **58**, 505 (1999).
[12] B. Anczykowski, J. P. Cleveland, D. Krüger, V. Elings, and H. Fuchs, Appl. Phys. A: Mater. Sci. Process. **A66**, S885 (1998).
[13] J. Tamayo, A. D. L. Humphris, A. M. Malloy, and M. J. Miles, Ultramicroscopy **86**, 167 (2001).
[14] W. Kauzmann, K. Moore, and D. Schultz, Nature (London) **248**, 447 (1974).
[15] P. Enoksson, G. Stemme, and E. Stemme, Sens. Actuators A **46–47**, 327 (1995).
[16] D. Westberg, O. Paul, G. I. Andersson, and H. Baltes, Sens. Actuators A **73**, 243 (1999).
[17] J. W. Berenschot, N. R. Tas, T. S. J. Lammerink, M. Elwenspoek, and A. van den Berg, J. Micromech. Microeng. **12**, 621 (2002).
[18] A short-term frequency stability of 30 mHz for a 390 kHz resonant beam is reported in D. Lange, C. Hagleitner, O. Brand, and H. Baltes, 14th Intl. Conf. Microelectromech. S., Interlaken, Switzerland, 2001, and a similar resolution at 33–72 kHz natural frequency but in a 60 Hz bandwidth has been demonstrated in T. R. Albrecht, P. Grütter, D. Horne, and D. Rugar, J. Appl. Phys. **69**, 668 (1991).